ISSN : 0974-7419 Volume 12 Issue 12

Trade Science Inc.

Analytical CHEMISTRY

An Indian Journal

Full Paper

ACAIJ, 12(12) 2013 [473-479]

OLA-NiO/MWCNTs/GC nanocomposite film modified electrode using simultaneous determination of acetaminophen and uric acid

D.Ranjith Kumar, D.Manoj, J.Santhanalakshmi*

Department of Physical Chemistry, University of Madras, Maraimalai Campus, Chennai-25, (INDIA)

E-mail: jslakshmi@yahoo.co.in

ABSTRACT

In the present work, we are reporting on the oleylamine capped nickel oxide (OLA-NiO) nanoparticles synthesized and are characterized by UV-vis, Furrier infra red spectroscopy, X-ray diffraction (XRD), Field emission scanning electron microscopy (FESEM) and high resolution transmission electron microscopic (HRTEM) analysis. From UV-vis spectra, the band gap energy of NiO nanopartilces was calculated to be 3.4 eV. The OLA-NiO nanoparticles fabricated on the surface of multi-walled carbon nanotubes (MWCNTs) modified glassy carbon electrode (GC). The obtained OLA-NiO/MWCNTs/GC modified electrode electrochemical behavior of acetaminophen (AC) and uric acid (UA) are investigated. In DPV, the OLA-NiO/MWCNTs/GC modified electrode shows a well defined oxidation peaks for AC and UA at +185mV and +264 mV. The modified electrode shows an improved sensitivity with better peak separation value up to 76mV and provides sufficient operational stability to simultaneous determination of AC and UA.

KEYWORDS

Nickel oxide nanoparticles;
X-ray diffraction;
Differential pulse voltammetry.

INTRODUCTION

Acetaminophen (N-acetyl-p-aminophenol, AC) serves as a widely used analgesic and non-steroid drug with moderate anti-inflammatory action[1]. An over dose and chronic therapy of AC can lead to toxic and acute fatal hepatoxicity and neprotoxicity[2,3]. Uric acid (2,6,8-trihydroxypurine, UA) and other oxypurines are the primary end products of purine metabolism in the human body[4,5]. High concentrations of UA in human body have been linked to many diseases such as gout, hyperuricaemia, Lesch-Nyan disease, obesity, diabetes, high cholesterol, high blood pressure, kidney disease and heart disease[6-8]. The determination of AC and UA usually coexist together and are considered as important molecules for physiological processes in human metabolism[9]. Therefore, the development of simple, a sensitive and selective method for the simultaneous determination of AC and UA is highly desirable for analytical applications and diagnostic researches. An important challenge is the simultaneous determination of AC and UA in which both AC and UA can be oxidized at the same potential on bare glassy carbon electrode (GC) resulting in a overlapping voltammetric response. Therefore, chemically modified electrodes can be widely used to resolve, to detect and to reduce the overpotential of the oxidizing species. There are more reports on the individual electrochemical determination of AC and UA reported[10]. The simultaneous determination of UA and AC using MWCNTs-chitosan modi-

Full Paper

fied GC electrode[11]. To a considerable effort there are no reports on the metal oxide nanoparticles modified electrode for the simultaneous determination of AC and UA. The modification of an electrode by nanostructured materials is an essential way to enhance the selectivity and sensitivity for the electrochemical determination of AC and UA. Therefore, in continuation of our recent studies the fabrication of OLA-NiO nanoparticles modified electrode was considered. Nickel oxide (OLA-NiO), a p-type semiconductor has been widely used in lithium ion batteries, fuel cells, electrochromic films, electrochemical super capacitors and biosensors[12-14]. The combinations of carbon nanotubes and metal oxide nanocomposite modified electrode have been widely used and their ability to promote electron transfer because of their high surface area, electrical conductivity and high chemical stability are well studied[15]. Thus in our present investigation, the asprepared OLA-NiO nanoparticles was fabricated on MWCNTs/GCE modified electrode which can provide an essential method to enhance the electron transfer properties of the OLA-NiO nanoparticles and increase the total electrocatalytic activity to lowering the detection limit and overpotential. The OLA-NiO/MWCNTs/GCE nanocomposite modified electrode offers an effective way to enhance the peak separation and sensitivity of AC and UA.

EXPERIMENTAL METHODS

Materials

Nickel(II)acetate tetrahydrate (Ni(OCO-$CH_3)_2.4H_2O$), 1-hexadecene, oleic acid, methanol, hexane, uric acid were purchased from Aldrich. Paracetamol tablets were obtained from local drug store. All of the chemicals and reagents used in the experiments were of analytical grade and used without further purification. Double distilled water (DD) was used in all experiments. A standard phosphate buffer (PBS) solution (pH-7.4) prepared with Na_2HPO_4 and NaH_2PO_4 was used as the supporting electrolyte.

Synthesis of OLA-NiO nanoparticles

The synthesis of OLA-NiO nanoparticles are adopted with early reported method[16]. In brief, nickel (II) acetate (10mmol) added to the mixture of oleylamine (6mL), dibenzyl ether (6mL) and tetralin (3mL), reaction mixture stirred with continues flow of N_2 gas. The temperature was slowly raised to 120°C to remove water. After that, the reaction mixer was further heated to 300°C and it was kept at this temperature for a few minutes. The obtained OLA-NiO nanoparticles products are washed with ethanol and dispersed in hexane for further characterization.

Fabrication of OLA-NiO/MWCNTs/GC modified electrode.

Before each experiment, GC surface was polished with increasingly finer grade alumina powders (1, 0.3 and 0.5 micron) down to mirror polish, sonicated for about 1 to 2 minutes in 1:1 nitric acid, degreased with acetone, washed with copious amount of DD water. 5mg of carboxyl functionalized MWCNTs and 2mg of OLA-NiO was dispersed in 3mL of (0.5%) ethanolic nafion solution by sonication for 30 min to get homogeneous black suspension. These colloids were dropped (5μL) onto GC and allowed to dry under ambient conditions obtained OLA-NiO/MWCNTs/GC modified electrode.

Instrumentation analysis

All the electrochemical measurements were performed on PGSTAT-12 electrochemical work station, (AUTOLAB, The Netherlands BV). The measurements were based on a three electrode system, with a glassy carbon electrode (GCE) of geometric area (0.07 cm^2), as a working electrode, a Pt wire with high geometrical surface area (~ 20 cm^2) as the counter electrode and saturated calomel electrode (SCE) as the reference electrode. In this work, functional groups are observed Tensor27 (Brucker). X-ray diffraction pattern (XRD) was collected on a Philips unit equipped with CuKα radiation source having 1.54A° unit wavelength. The high resolution transmission electron microscopy (HRTEM) images were obtained from TECNAI-G^2 (model T- 30).

RESULTS AND DISCUSSION

UV-vis spectra of OLA-NiO nanoparticles

Figure 1 shows the absorbance spectra for OLA-NiO nanoparticles. For a direct band gap semiconductor, the absorbance in the vicinity of the onset due to the electronic transition is given by the following Eq. 1.

$$(\alpha h\nu)^n = K(h\nu - E_g) \quad (1)$$

where, hν is the photon energy, α is the absorption coefficient, E_g is the band gap energy, and *n* is either 2 for a direct transition or ½ for an indirect transition. The plot of $(\alpha h\nu)^2$ vs hν based on the direct transition are shown in Figure 1 (Inset). The extrapolated value (the straight lines to the x axis) of E_g at α =0 gives absorption edge energies corresponding to E_g= 3.4eV, which is in good agreement with the reported value for the direct band gap[17].

FTIR spectra

The Figure 2(a) shows the FTIR spectra of pure oleylamine and oleylamine capped NiO nanoparticles.

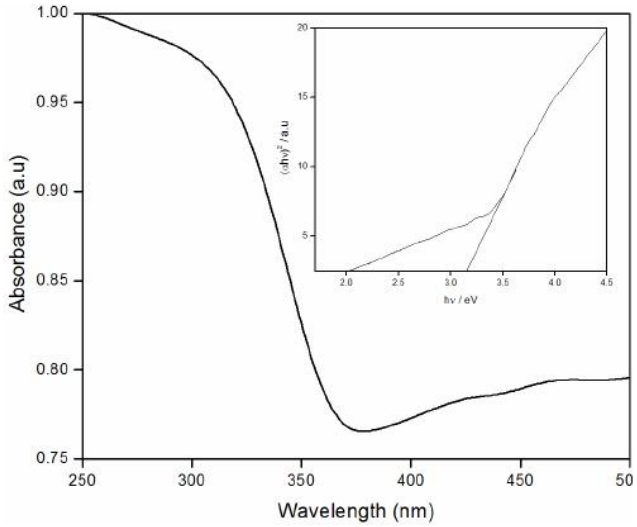

Figure 1 : UV-vis spectrum of the OLA-NiO nanoparticle. The inset shows plot of $(\alpha h\nu)^2$ vs photon energy.

In the characteristic N-H bending vibration band appeared at 1561 cm^{-1} and the N-H stretching vibrations of weak and broad bands at the range of 3000-3300 cm^{-1}. The bands at 2850 and 2928 cm^{-1} are attributed to the asymmetric CH_2 stretch and the symmetric CH_2 stretch in oleylamine, respectively, and the band at 1409 cm^{-1} corresponded to the CH_3 umbrella mode of oleylamine[18]. Figure 2(b) shows the Oleylamine capped NiO nanoparticles, it clearly indicate slight red shift in asymmetric CH_2 stretch and the symmetric CH_2 and also the N-H stretching slight blue shift are resulted formation of a relatively close-packed Oleylamine on NiO nanoparticles[19]. The characteristic Ni-O nanoparticles stretching bond at 424 cm^{-1}[20].

X-ray diffraction

Figure 3 shows the XRD pattern of oleic acid stabilized NiO nanoparticles and shows sharp diffraction

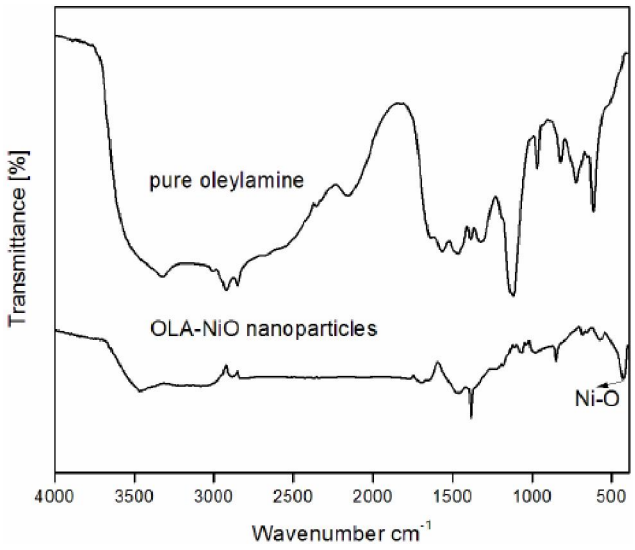

Figure 2 : FTIR spectra of (a) pure oleylamine, (b) Oleylamine capped NiO nanoparticles.

peaks at 2θ=37.30, 43.39, 63.01, 75.48, and 79.61 which are associated with (111), (200), (220), (311), and (222) agrees well with the standard diffraction pattern (JCPDS card No. 78-0429)[21]. The NiO reflections can be indexed as *face-centered cubic* (*fcc*), From the XRD analysis, there is no impurity peak observed which indicates the formation of pure NiO only. The particle size calculated using Scherrer equation was found to be 19 nm.

HRTEM image of OLA-NiO nanoparticles

Figure 4(A) shows a representative high resolution transmission electron microscopy (HRTEM) image of

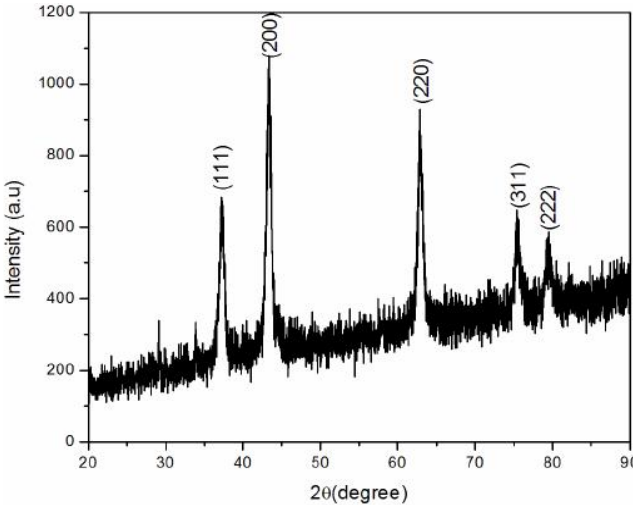

Figure 3 : XRD pattern of OLA-NiO nanoparticles.

the OLA-NiO nanoparticles obtained the average particle size are calculated to be 2.5±0.5nm. It can be seen

Full Paper

that the OLA-NiO nanoparticles possess a nearly narrow size distribution and consist of a pure OLA-NiO nanoparticles (Figure (4B). The dibenzyl ether, tetralin and Oleylamine were employed as solvents and capping agents play important in OLA-NiO nanoparticles grew up then NiO capped by Oleylamine effectively. In this, the lower energy barrier favors the heterogeneous nucleation of the OLA-NiO nanoparticles. Energy-dispersive X-ray spectroscopy mapping results (Figure 3C) further confirm the composition of Ni and O nanoparticles[16].

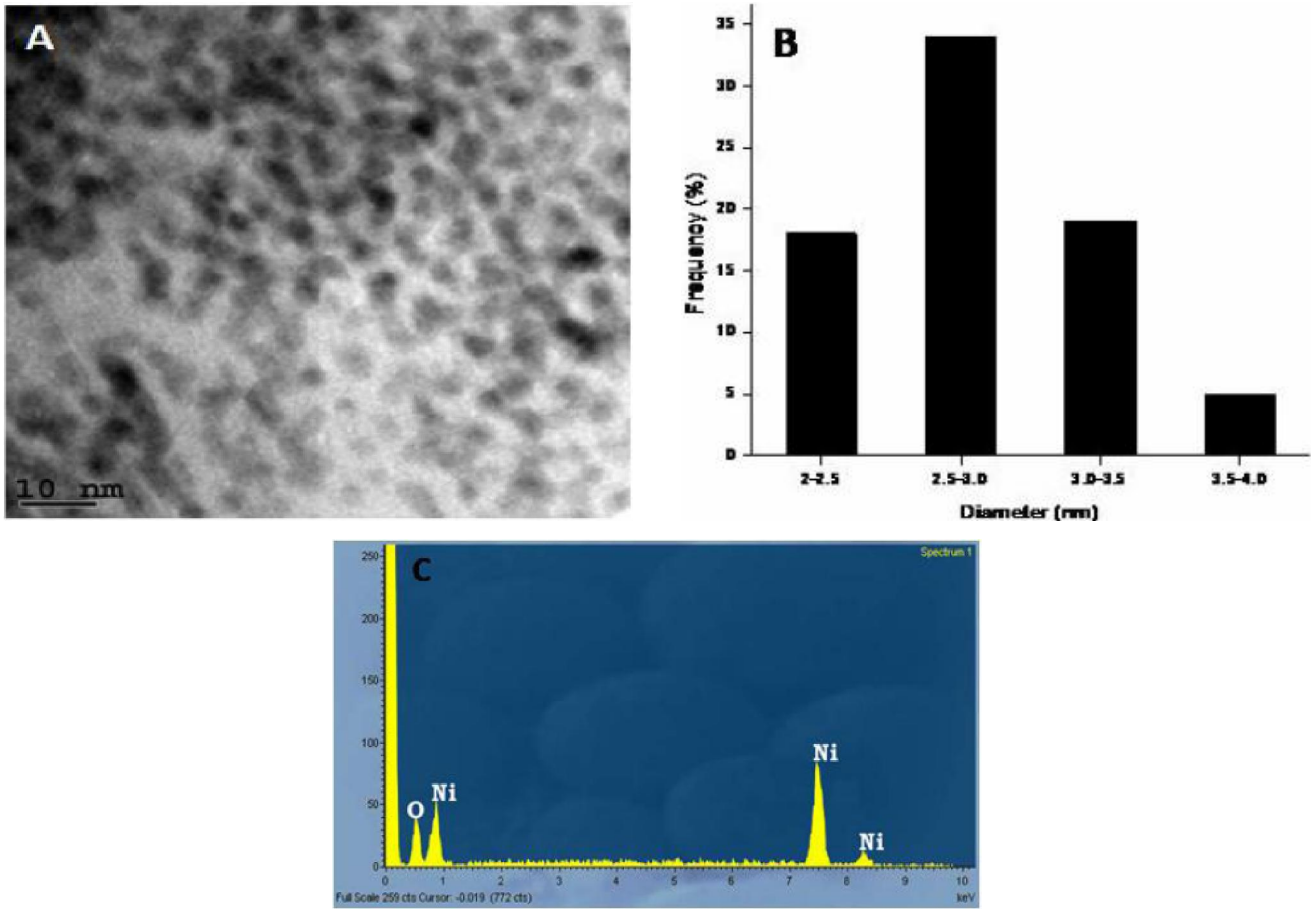

Figure 4 : (a) HRTEM images of OLA-NiO (b) corresponding particle size distributions of nanoparticles (c) Representative EDX pattern of OLA-NiO nanoparticles.

Morphology study of OLA-NiO/MWCNTs/GC composite

Figure 5 shows the (A) bare GC surface, (B) acid functionalized MWCNTs/GC surface and (C) OLA-OLA-NiO/MWCNTs/GC composite. In the OLA-NiO/MWCNTs/GC composite OLA-NiO nanoparticles Oleylamine surface amine group are electrostatically adsorbed on the acid functionalized MWCNTs acid group sites. This electroctrostatic interaction between nanoparticles and MWCNTs leads to the stability of modified electrode and electron transfer of analyte and electrode surface.

Electrochemical impedance study of OLA-NiO/MWCNTs/GC modified electrode

EIS was employed to further investigate OLA-NiO/MWCNTs/GC modified electrode surface. Figure 6 shows the results of the EIS at bare GC, MWCNTS/GC (Figure 6 inset) and OLA-NiO/MWCNTs/GC in the presence of 2mM $[Fe(CN)_6]^{4-}$ with 0.1M phosphate buffer solution (pH-7). The resistance exhibits the electron transfer kinetics of the redox-probe at bare electrode interface in Figure 6(a) there is a high charge transfer resistance for $[Fe(CN)_6]^{4-}$ at bare. The results for OLA-NiO/MWCNTs/GC modified electrodes shown in Figure 6(b), the Rct values were decreased to bare GC 782Ω, and OLA-NiO/MWCNTs/GC is very low charge transfer resistance 646Ω. The Rct value of OLA-NiO/MWCNTs/GC modified electrode with bare GC de-

creased markedly to approximately 136Ω and indicating that OLA-NiO have good conductivity and that the OLA-NiO/MWCNTs/GC electrode can make the electron transfer easier.

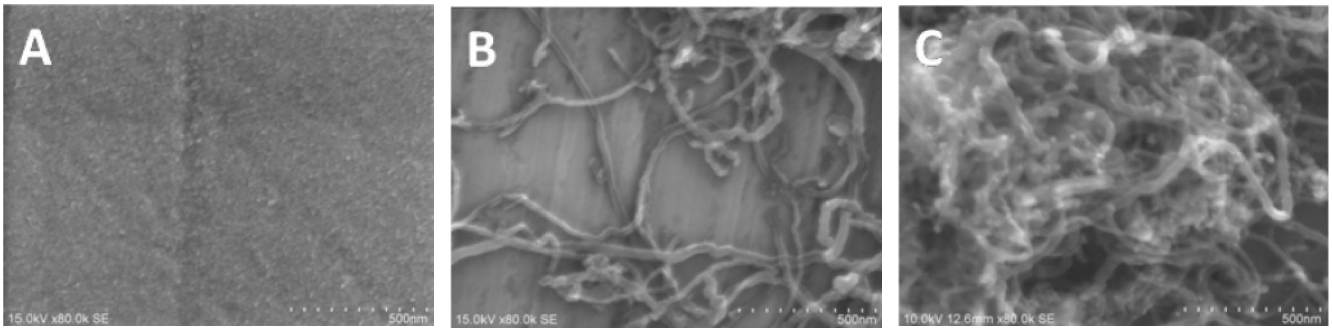

Figure 5 : (A) Bare GC (B) MWCNTs/GC (C) OLA-NiO/MWCNTs/GC

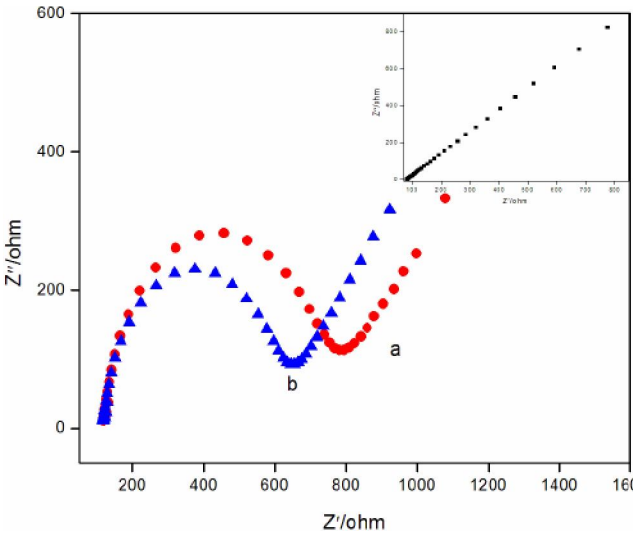

Figure 6 : Impendence plots of bare GC (curve a), MWCNTs/GC (curve b), and OLA-NiO/MWCNTs/GC (curve c) electrodes in the presence of 2mM $Fe(CN)_6^{3-/4-}$ with 0.1M PBS in (pH-7) as supporting electrolyte. The electrode potential was 0.178V; the frequency range was 1 Hz to 100 KHz.

the mixtures of 20µM AC and 0.1mM UA in 0.1M PBS (pH-7.4) at a scan rate of 50mVs^{-1}. At the bare GC, there is no significant current response for UA and AC is observed. However, MWCNTs/GC electrode shows oxidation peak for UA and AC but there is no peak separation are observed. In contrast to the bare GC and MWNCTs/GC, the OLA-NiO/MWCNTs/GC electrode shows two oxidation peaks at +220 and +280 mV with enhanced peak current for UA and AC respectively. Also, the anodic peak experiences a shift towards negative potential which indicates the OLA-NiO nanoparticles decreased the overpotential for UA and AC. The OLA-NiO/MWCNTs/GC modified electrode shows a better peak separation value of 76mV which

Electrochemical determination of UA and AC at OLA-NiO/MWCNTs/GC modified electrode

Figure 7 shows the cyclic voltammograms (CV) of

indicates the presence of OLA-NiO nanoparticles is responsible for electron transfer on the electrode surface. The enhanced oxidation peak current of AC and UA at NiO/MWCNTs/GC modified electrode is attributed to the increased effective mass transport and surface area of the NiO nanoparticles on the electrode surface. Thus OLA-NiO/MWCNTs/GC modified electrode is a better counterpart than MWCNTs/GC and bare GC.

Effect of scan rates

Figure 8 shows the CVs OLA-NiO/MWCNTs/GC modified electrode in 0.1mM UA in pH-7.4(PBS 0.1M) at different scan rates ranging from 10-250mVs^{-}

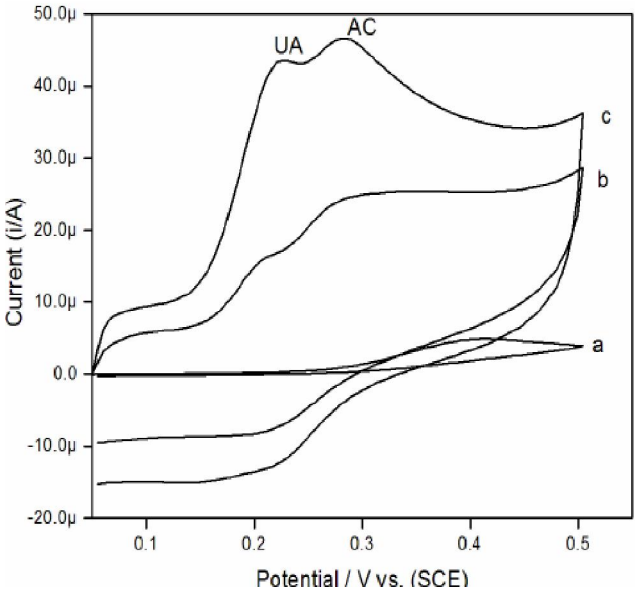

Figure 7 : CVs response for the mixture of 20µM AC + 0.1mM UA at bare GCE (a), MWCNTs/GCE (b) and NiO/MWCNTs/GCE (c) modified electrode at a scan rate of 50 mV s^{-1} in 0.1 M PBS (pH-7.4).

Full Paper

[1]. The peak current increased linearly with increase in scan rate (Figure 8A Inset) with a linear regression of Ipa = 0.367+6.134ν, R^2 = 0.994. This indicates the adsorption of uric acid molecules on electrode surface. It is further confirmed with the double lograthamic plot (Figure 8B) with a slope value of 0.9 which indicates the adsorption of uric acid molecules on the electrode surface. Based on the Laviron equation[22], the electron transfer coefficient was evaluated to be 0.52 and the electron transfer rate constant k_s are $3.7s^{-1}$. The calculated k_s show that the resultant electrode can facilitate the electron transfer on OLA-NiO/MWCNTs/GC electrode.

Simultaneous determination of UA and AC on OLA-NiO/MWCNTs/GC modified electrode.

The objective of present work was the improvement of a UA oxidation and peak separation of electrochemical responses of UA and AC. The utilization of the OLA-NiO/MWCNTs/GC modified electrode for the simultaneous determination of UA and AC was demonstrated by simultaneously varying the concentrations of UA and AC. From the DPV results show the two well defined oxidation peaks with a peak separation value of 76mV as shown in the Figure 9. The anodic peak currents increase linearly with increase in both concentration of UA and AC from the range of 42.8μM to 179.7μM UA and 2.9μM to 10.0μM AC respectively. Sensitivity was calculated from the linear calibration plot on the above range slope of 0.011and 0.415μAμM^{-1} for UA and AC. The limit of detection (LOD) value was calculated to be 35 μM and 1.38μM

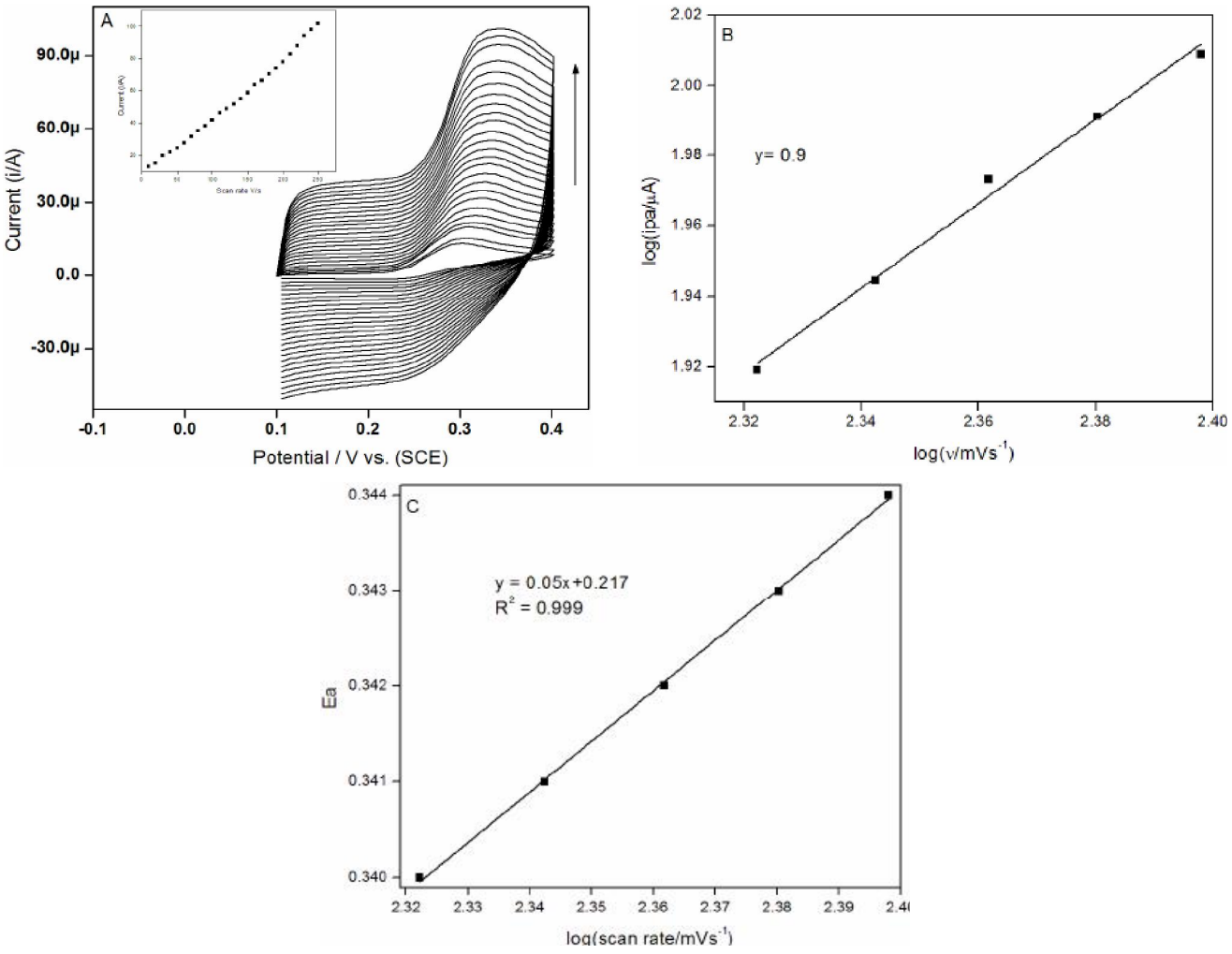

Figure 8 : CVs on 0.1mM UA in 0.1M PBS solution on OLA-NiO/MWCNTs/GCE at different scan rates: (10-250mVs^{-1}. Inset (A): The plot of peak current vs. scan rate. (B) The plot of logarithm of ipa vs. logarithm of scan rates. (C) Ea vs logarithm υ

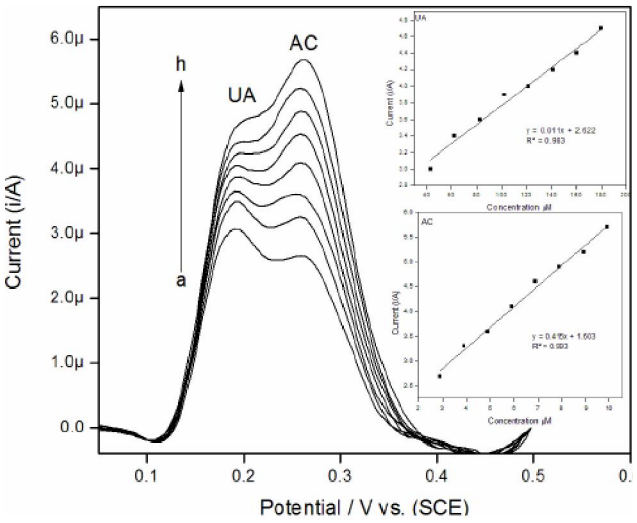

Figure 9 : DPVs of in 0.1M PBS (pH 7.4) containing different concentrations of UA and AC: mixed solutions of 42.8 + 2.9, 62.6 + 3.9, 82.6 + 4.9, 101.9 + 5.9, 121.5 + 6.9, 140.9 + 7.9, 160.3 + 8.9 and 179.7 + 9.9μM. Insets: calibration plot for the increasing concentration of UA and AC vs anodic peak currents of UA and AC.

for UA and AC respectively.

CONCLUSION

In summary, OLA-NiO nanoparticles were prepared by effective thermolysis in high boiling point solvent medium. The as synthesized OLA-NiO nanoparticles are characterized with UV-vis, FTIR and XRD. In the presence of OLA-NiO nanoparticles is responsible for the enhanced performance for the electrochemical oxidation of AC and UA in physiological conditions. OLA-NiO/MWCNTs/GC modified electrode shows enhanced the peak separation with better sensitivity and limit of detection for AC and UA.

ACKNOWLEDGMENT

Financial support from National centre for Nanoscience and Nanotechnology (NCNSNT), University of Madras, Chennai is gratefully acknowledged by the authors.

REFERENCES

[1] Y.Shi, L.Zhang, R.Jiang, W.Chen, W.Zheng, L.Chen, L.Tang, L.Li, L.Li, W.Tang, Y.Wang, Y.Yu; Int.Immunopharmacol., **14**, 530 **(2012)**.
[2] C.G.Antoniades, A.Quaglia, L.S.Taams, R.R.Mitry, M.Hussain, R.Abeles, L.A.Possamai, M.Bruce, M.McPhail, C.Starling, B.Wagner, A.Barnardo, S.Pomplun, G.Auzinger, W.Bernal, N.Heaton, D.Vergani, M.R.Thursz, J.Wendon; Hepatology., **56**, 735 **(2012)**.
[3] D.J.Antoine, R.E.Jenkins, J.W.Dear, D.P.Williams, M.R.McGill, M.R.Sharpe, D.G.Craig, K.J.Simpson, H.Jaeschke, B.K.Park; J.Hepatol., **56**, 1070 **(2012)**.
[4] M.J.Kuchan, K.M.Ostrom, C.Smith, P.E.Hu; J.Am Coll Nutr., **19**, 16 **(2000)**.
[5] A.J.Clifford, J.A.Riumallo, V.R.Young, N.S.Scrimshaw; J.Nutr., **106**, 428 **(1976)**.
[6] J.C.K.Mbouguen, I.T.Kenfack, A.Walcarius, E.Ngameni; Talanta., **85**, 754 **(2011)**.
[7] H.Beitollahi, I.Sheikhshoaie; Electrochim.Acta., **56**, 10259 **(2011)**.
[8] H.Beitollahi, J.B.Raoof, R.Hosseinzadeh; Electroanalysis., **23**, 1934 **(2011)**.
[9] Y.Wang; Colloids Surf.B., **88**, 614 **(2011)**.
[10] G.Hu, L.Chen, Y.Guo, X.Wang, S.Shao; Electrochim.Acta, **55**, 4711 **(2010)**.
[11] A.Babaei, D.J.Garrett, A.J.Downard; Electroanalysis., 23417 **(2011)**.
[12] G.Natu, P.Hasin, Z.Huang, Z.Ji, M.He, Y.Wu; ACS Appl.Mater.Interfaces, **4**, 5922 **(2012)**.
[13] S.Farhadi, Z.R.Zaniyani; Polyhedron., **30**, 971 **(2011)**.
[14] B.Zhao, J.Song, P.Liu, W.Xu, T.Fang, Z.Jiao, H.Zhang, Y.Jiang; J.Mater.Chem., **21**, 18792 **(2011)**.
[15] N.Chopra, W.Shi, A.Bansa; Carbon., **49**, 3645 **(2011)**.
[16] P.Li, Z.Wei, T.Wu, Q.Peng, Y.Li; J.Am.Chem.Soc., **133**, 5660 **(2011)**.
[17] W.J.Duan, S.H.Lu, Z.L.Wu, Y.S.Wang; J.Phys.Chem.C, **116**, 26043 **(2012)**.
[18] J.He, P.Kanjanaboos, N.L.Frazer, A.Weis, X.M.Lin, H.M.Jaeger; Small., **6**, 1449 **(2010)**.
[19] O.Chen, Y.Yang, T.Wang, H.Wu, C.Niu; J.Yang, Y.C.Cao; J.Am.Chem.Soc., **133**, 17504 **(2011)**.
[20] J.Li, R.Yan, B.Xiao, D.T.Liang, D.H.Lee; Energy & Fuels, **22**, 16 **(2008)**.
[21] M.N.Mancheva, R.S.Iordanova, D.G.Klissurski, G.T.Tyuliev, B.N.Kunev; J.Phys.Chem.C, **111**, 1101 **(2007)**.
[22] E.Laviron; J.Electroanal.Chem., **101**, 19 **(1979)**.